Forecasting Probabilistic Seismic Shaking for Greater Tokyo from 400 Years of Intensity Observations

Serkan B. Bozkurt,[a),b)] Ross S. Stein,[a)] and Shinji Toda[c)]

The long recorded history of earthquakes in Japan affords an opportunity to forecast seismic shaking exclusively from past shaking. We calculate the time-averaged (Poisson) probability of severe shaking by using more than 10,000 intensity observations recorded since AD 1600 in a 350 km-wide box centered on Tokyo. Unlike other hazard-assessment methods, source and site effects are included without modeling, and we do not need to know the size or location of any earthquake nor the location and slip rate of any fault. The two key assumptions are that the slope of the observed frequency-intensity relation at every site is the same, and that the 400-year record is long enough to encompass the full range of seismic behavior. Tests we conduct here suggest that both assumptions are sound. The resulting 30-year probability of $I_{JMA} \geq 6$ shaking ($\sim$PGA ≥ 0.4 g or MMI $\geq$ IX) is 30%–40% in Tokyo, Kawasaki, and Yokohama, and 10%–15% in Chiba and Tsukuba. This result means that there is a 30% chance that 4 million people will be subjected to $I_{JMA} \geq 6$ shaking during an average 30-year period. We also produce exceedance maps of PGA for building-code regulations, and calculate short-term hazard associated with a hypothetical catastrophe bond. Our results resemble an independent assessment developed from conventional seismic hazard analysis for greater Tokyo. [DOI: 10.1193/1.2753504]

INTRODUCTION

Our goal is to conduct a probabilistic seismic hazard analysis that is driven to the greatest extent possible by observations, and is as free as possible of modeling assumptions. Such an approach is best suited to regions where the record of earthquake shaking is long, and the reporting of the shaking is reliable and consistent through time. Although beneficial, we will argue that the earthquake rate need not be high for such a method to succeed.

For different parts of the world, there have been many complex and detailed seismic hazard-assessment studies that have utilized the current knowledge and observations. Each of the myriad elements of these traditional probabilistic seismic hazard analyses contains uncertainty, and so despite their sophistication the final product inevitably suffers from a large combined uncertainty that is difficult to assess fully, and nearly impos-

[a)] U.S. Geological Su30rvey, MS 977, 345 Middlefield Road, Menlo Park, CA 94025
[b)] Geomatrix Consultants, Inc., 2101 Webster Street, CA 94612
[c)] Active Fault Research Center, AIST, Site 7, 1-1-1 Higashi, Tsukuba, Ibaraki, 205-8567 Japan

Earthquake Spectra, Volume 23, No. 3, pages 525–546, August 2007;

Table 1. Sources of intensity data used in this study

Time period	Data source	Number of $I_{JMA} \geqslant 3$ observations
1600-1884	Usami (1994)	1,579
1885-1922	Utsu (1979) and Usami (2003)	377
1923	Hamada et al. (2001) and Takemura and Moroi (2001)	1,187
1924-1925	Utsu (1979) and Usami (2003)	30
1926-2000	JMA (2002)	7,243
1600-2000	Total	10,416

sible to test. This is why an independent approach to corroborate or validate seismic hazard assessment, as we seek here, is valuable. Stirling and Peterson (2006) used the frequency of historical intensity data to validate probabilistic analyses for a number of cities in New Zealand and the United States, and found the two methods to give comparable results in most cases. On a smaller scale and using similar methods, intensities have been used to make probabilistic hazard analyses for several cities in Italy (Monachesi et al. 1994, Papoulia and Slejko 1997). In this paper we utilize a much larger and more complete data set over a 300-km $\times$ 300-km region to investigate and depict the spatial distribution of ground shaking.

Fortunately, the great seismologist Tatsuo Usami gathered and codified the historical record of earthquake effects in Japan as his life's work. In addition, studies by Utsu (1979), Takemura and Moroi (2001), Hamada et al. (2001), and JMA (2004) greatly enhanced this trove of data for more recent periods. We digitized, combined, and analyzed these data (Table 1). Virtually the entire Kanto plain on which Tokyo sits has been subjected to $I_{JMA} \geqslant 6$ (equivalent to Modified Mercalli Intensity [MMI] $\geqslant$ IX) shaking at least once since Edo (today's Tokyo) was first settled in 1603 (Figure 1a). Much of the strongest shaking is associated with three large shocks, the 1703 M $\sim$ 8.2 Genroku, 1855 M $\sim$ 7.2 Ansei-Edo, and 1923 M = 7.9 Kanto earthquakes (Figure 1b–1d). The 1703 and 1923 shocks struck on the Sagami trough megathrust at shallow depth (Nyst et al. 2006, Shishikura et al. 2006), whereas the 1855 shock probably occurred beneath Chiba at much greater depth (Bakun 2005, Grunewald and Stein 2006; Figure 1b–1d). The peak intensity we report for the Kanto region is in substantial agreement with the compilation by Miyazawa and Mori (2005) for all of Japan.

INTENSITY DATABASE

The Usami (1994) and JMA (2004) catalogs span 82.5% of the time period, and thus form the backbone observations (Table 1). Unfortunately, the observations from which Utsu (1979) drew intensity contour maps for earthquakes during 1885–1922 are unpublished and unavailable. Since most of the observations in the Usami and Utsu catalogs were referenced to the modern JMA scale (Table 2), we also use the JMA scale. On the basis of the observed frequency-intensity relationship that we will present in the next

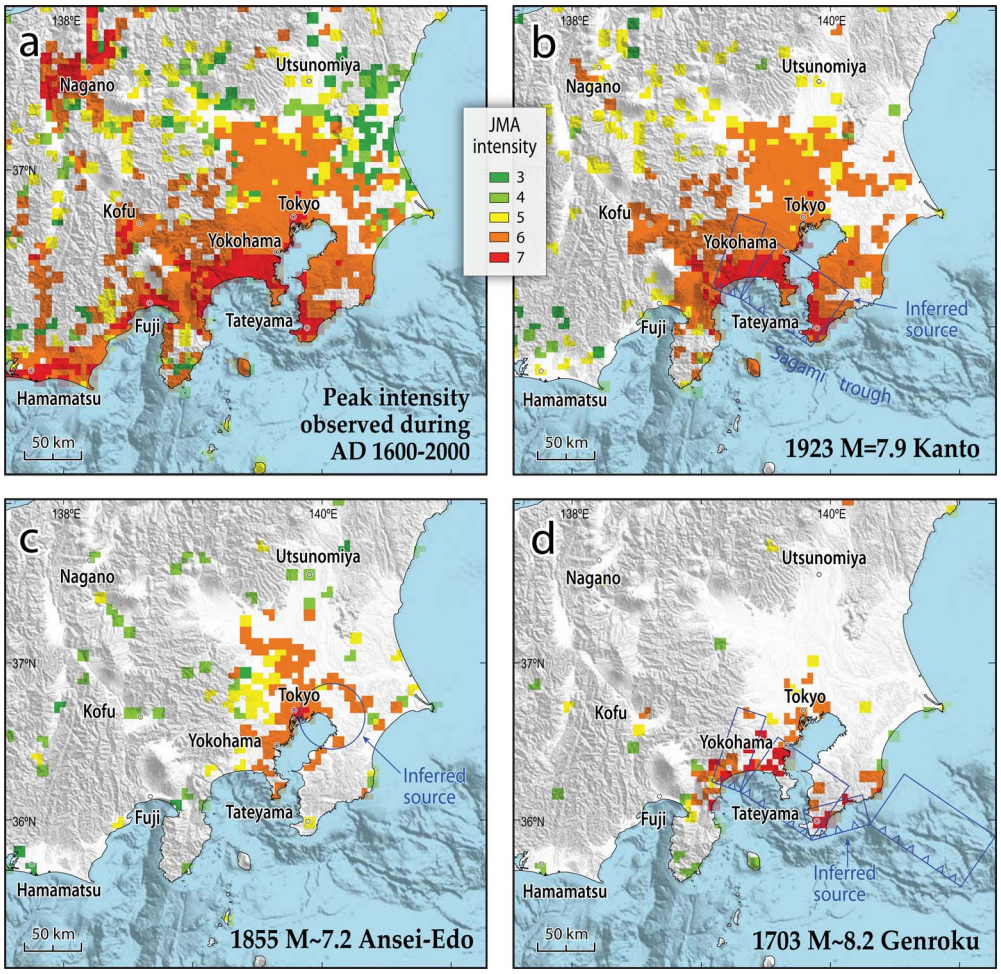

Figure 1. Maps of earthquake intensities observed within 5- × 5-km cells. (a) Peak intensity for the entire catalog duration. (b–d) Intensity distribution for the three largest earthquakes recorded during the 400-year period, with sources inferred by Nyst et al. (2006) for 1923, Grunewald (2006) for 1855, and Shishikura et al. (in preparation) for 1703.

section, we judge the catalog to be clearly incomplete for $I_{JMA} < 3$ and possibly incomplete at $I_{JMA} = 3$, and so $I_{JMA} < 3$ data were excluded. Table 2 describes the principal felt effects and building damage employed to assess intensity. Fujimoto & Midorikawa (2005) used a set of earthquakes with both intensity observations and strong ground motion records to deduce the peak ground acceleration (PGA) and peak ground velocity (PGV) associated with the JMA intensities; this equivalence makes the intensity data considerably more useful for engineering applications. Because intensities were historically measured in one- to three-story wood and masonry houses, they are principally sensitive to accelerations in the 6 ± 2 Hz frequency range (ICBO 1997).

Table 2. Explanation of JMA seismic-intensity scale and ground motion equivalents

Observations used to assess shaking intensity	JMA intensity	Estimated peak ground acceleration	Estimated peak ground velocity	Modified Mercalli intensity
Felt by most people in the building: some people are frightened.	3	~0.02 g	~0.02 m/s	~III–IV
Many people are frightened: some people try to escape from danger, most sleeping people awaken.	4	~0.08 g	~0.07 m/s	~V–VI
Occasionally, less earthquake-resistant houses suffer damage to walls and pillars.	5 lower	~0.14 g	~0.11 m/s	
	5	~0.25 g	~0.19 m/s	~VI–VIII
Occasionally, less earthquake-resistant houses suffer heavy damage to walls and pillars, and lean.	5 upper	~0.41 g	~0.34 m/s	
Occasionally, less earthquake-resistant houses collapse, and even walls and pillars of highly earthquake-resistant houses are damaged.	6 lower	~0.41 g	~0.34 m/s	
	6	~0.65 g	~0.63 m/s	~IX–X
Many less earthquake-resistant houses collapse. In some cases, even walls and pillars of highly earthquake-resistant houses are heavily damaged.	6 upper	~1.02 g	~1.21 m/s	
Occasionally, even highly earthquake-resistant houses are severely damaged, and lean.	7	>1.02 g	>1.21 m/s	~XI–XII
Source: Japan Meteorological Agency (2004)		Source: Fujimoto & Midorikawa (2005)		Shabestaria & Yamazaki (2001)

In 1996, JMA introduced a decimal seismic-intensity scale calculated from acceleration records produced by seismic-intensity meters calibrated to match the historical scale. Currently, JMA operates a network of 180 seismographs and 600 seismic-intensity meters, and collects data from nearly 2,800 seismic-intensity meters operated by local governments. We use the JMA intensity meter data, rounded to the JMA scale divisions shown in Table 2, in our observations. For comparison, the widely used MMI scale (Richter 1958) is also shown.

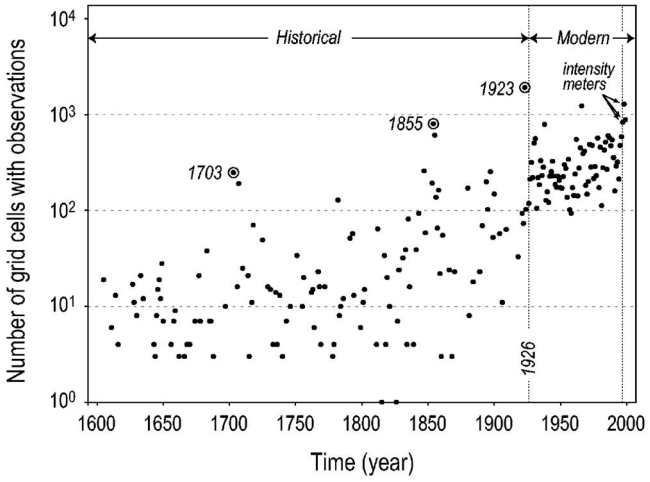

Figure 2. The long-term increase in the number of cells with intensity observations and the large number of cells for the three largest earthquakes are evident. After 1926, the JMA systematically recorded earthquake intensities.

We have placed the complete data available online in both GIS and text formats at http://earthquake.usgs.gov/research/modeling/intensities/.

MODERN AND HISTORICAL PERIODS

We divided our catalog into the historical period covering AD 1600 to 1925, drawn largely from Usami (1994) and Takemura and Moroi (2001), and the modern period covering 1926 to 2000, which is based on JMA (2004). Although both periods contain spatially rich data, the observation abundance and completeness differ (Figure 2). Fortunately, the two periods furnish complementary data. The historical period includes large destructive earthquakes, such as those in 1703, 1855, and 1923, but poorly samples low-intensity shaking (Table 1). Because the largest event to strike during the modern period was a swarm of several $M \geqslant 7$ earthquakes in 1938, the modern catalog includes few high intensities, but is rich in low-intensity observations.

METHODOLOGY

We carried out the analysis in a geographic information system (GIS) linked to a large spreadsheet. This permitted us to manipulate and plot maps of the 10,000 observations in 2,000 cells, to readily test different assumptions on the resulting probabilities, and to overlay this information with geologic, geographic, and population data.

DATA DIGITIZATION

Although the post-1926 JMA intensity catalog includes latitude and longitude information along with the intensity observations, observation locations for Usami and Utsu historical catalogs are not sufficiently accurate to digitize. As shown in Figure 3, the

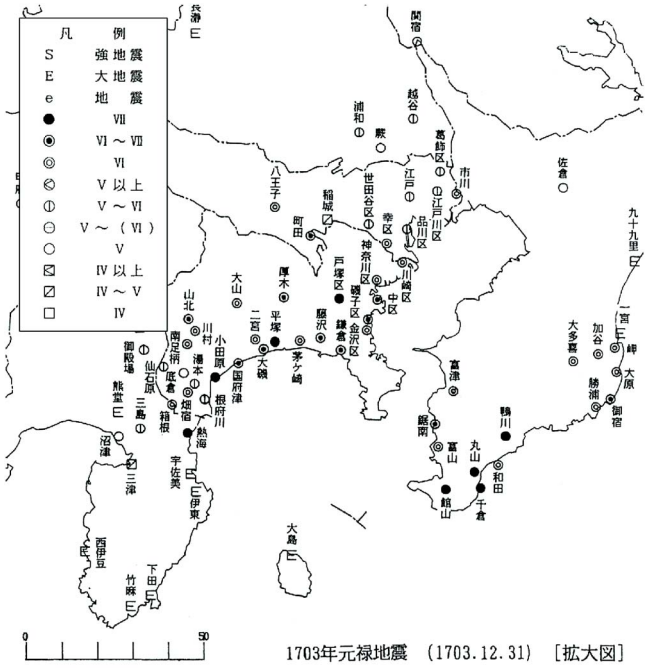

Figure 3. An example of an earthquake-intensity map from Usami (1994), for the 1703 M ~8.2 Genroku earthquake. The symbols depict intensity levels; the characters above the symbols denote town names.

maps from which we work show an intensity symbol beneath a location name. So, rather than digitize these maps, we cross-referenced the ancient location names with several modern and ancient maps to assign coordinates to the observations. We also converted the mapped intensity symbols into numerical values using Usami's descriptions. We assigned observations in the Usami maps described as intensity ranges, such as "I_{JMA} 5 to 6" to $I_{JMA}=5.5$; "I_{JMA} 5 or larger" was converted to $I_{JMA}=5.25$.

We followed a similar approach for Utsu observations for 1885–1925. $I_{JMA} \geq 3$ intensities reported by Usami (2003) were digitized as previously described, but for most earthquakes during this time period, we have only interpolated intensity contours (Utsu 1979, Utsu 1982, Utsu 1988, Usami 2001). So we digitized the contours at sites where we also have JMA intensity data for the 1923 Kanto earthquake. Thus the natural variability and inconsistency of the observations is lost. Fortunately, few large earthquakes struck during this period, and the 1923 JMA site coverage was sparse. So at worst, we undersample intensities during 1885–1925.

We use three data sources for the 1923 Kanto earthquake and the first three months of aftershocks. The digital JMA catalog intensities were directly imported to the GIS. The 1923 JMA catalog, however, includes little data where destruction was near total, such as along the Tokyo-Yokohama corridor. To fill this gap and enhance the spatial sampling, we also included an intensity map published by Takemura and Moroi (2001). Be-

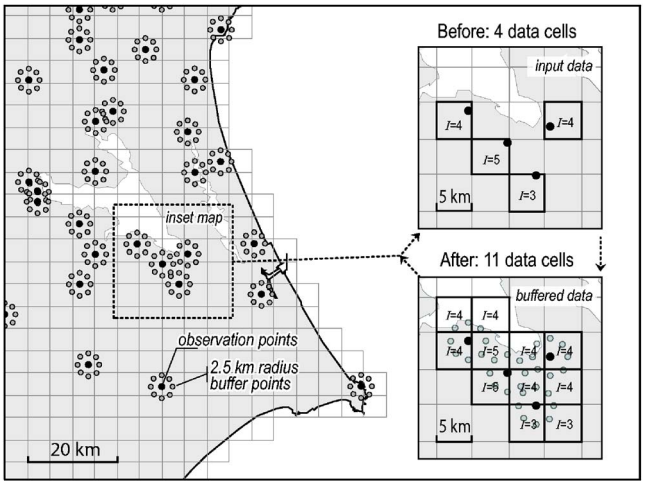

Figure 4. Intensity observations (black dots) are buffered, a form of smoothing (gray dots) so that more cells (squares) contain observations, making the resulting cell intensities less sensitive to location errors.

cause the Takemura and Moroi (2001) data were not made available to us in digital format, we digitized the center point of each township for which intensity was assigned (ranging from 2-km × 2-km to 10-km × 15-km areas), including JMA stations where available. Finally, Hamada et al. (2001) published aftershock intensities recorded at all JMA and several other seismic observatories for the three months after the 1 September 1923 earthquake. The aftershock data have high temporal and low spatial sampling.

GRIDDING AND BUFFERING

We divided our study region into 5-km × 5-km cells for mapping and statistical analysis. Cell size trades off observation density with spatial coverage. We chose a cell size to capture the scale of geologic features that influence site amplification, such as the width of streambeds and the extent of soft sediments that rim Tokyo Bay. Further, the bias created by the much more densely sampled 1923 and 1854 earthquakes is minimized, as multiple observations in each cell are averaged. Although intensity observations are stored as points, they represent shaking recorded in a town or village. Thus, to smooth the data we applied a radius buffer of half the cell width, or 2.5 km, to each observation point (Figure 4). This method also helped us to minimize location uncertainty of historic observations. As shown in Figure 4, the buffering causes stations near cell borders to influence adjacent cells, and so the total number of cells with data increases.

REGIONAL FREQUENCY-INTENSITY CURVE

We combine observations from all cells to find a regional frequency-intensity distribution. This is similar to calculating a *b*-value from a frequency-magnitude distribution,

with intensity replacing magnitude. As shown in Figures 2 and 5a, the modern portion of the catalog has few $I_{JMA} \geqslant 6$ observations simply because there have been few large earthquakes in the area during this period; the historical portion is incomplete for $I_{JMA} \geqslant 5$ due to incompleteness at low intensities. We have excluded the incomplete data in the historical catalog and merged the remainder.

The data are well fit by an exponential decay curve (Figure 5b). Although a power-law curve might be expected for the attenuation of strong ground motion with distance, intensity assignments are based on damage descriptions and thus are not strictly scaled numerically, and so the relation need not be power-law.

There are two reasons for such an observed decay relation, earthquake abundance, and seismic attenuation: First, similar to a *b*-value plot, there are many more small earthquakes than large ones. Second, there are many more epicenters far from a given observation station than close to it. Thus observations of weak shaking are far more common than strong shaking. In Figure 5c, we assume a *b*-value of 1.0, as found for the Kanto region by Grunewald and Stein (2006). Next, we randomly distribute 1 million $5 \geqslant M \geqslant 8$ earthquake sources over the Kanto area, extracting 400-year periods by Monte Carlo simulation. Finally, we use the intensity attenuation relations developed for the Kanto region by Bakun (2005). Although Bakun (2005) finds a linear relation between magnitude and intensity, the log-distance term dominates. When one combines the log-distance dependence with the power-law dependence of earthquake frequency with magnitude (the *b*-value), one finds the exponential relation between frequency and intensity we show here. The resulting theoretical frequency-intensity relations are in close agreement with the observations, particularly if most earthquakes occur in the crust.

APPLYING THE REGIONAL SLOPE TO LOCAL CELLS

We assume that the regional decay slope applies to each individual cell, but allow the intercept to vary in each cell. In other words, the ratio of strong to weak shaking is taken as constant, but the frequency of shaking is permitted to vary. This permits us to calculate earthquake probabilities for cells that contain only a few observations because we are only solving for the intercept (or frequency). This approach is consistent with independent observations that the spatial variability of *b*-values is smaller than variations in earthquake rate (Wiemer and Wyss 1997). In Figure 6, we test how the exponential decay curve satisfies observations for eight cities with cells containing a large number ($N_{IJMA}=50-400$) of observations, and for two cities with a small number of observations ($N_{IJMA}=4-8$). Regression coefficients (R^2) for the six cells with plentiful observations range from 0.88–0.99, and the least squares (Π) misfit ranges from 0.17–0.01, indicative of good fits to the observations. Yokohama, with 256 observations, yields nearly the same probability as West Yokohama, with only eight observations 15 km away. We thus use the frequency-intensity curve to estimate the frequency of shaking at any intensity level. The merit of this approach is that for a frequency estimate at, for example, $I_{JMA}=6$, the estimate uses all the data, not just the $I_{JMA}=6$ observations. In fact, $I_{JMA}=6$ observations are not required to make an estimate if the curve is well fit. In this way, effects of historical data incompleteness or the bias generated by large earthquakes are minimized.

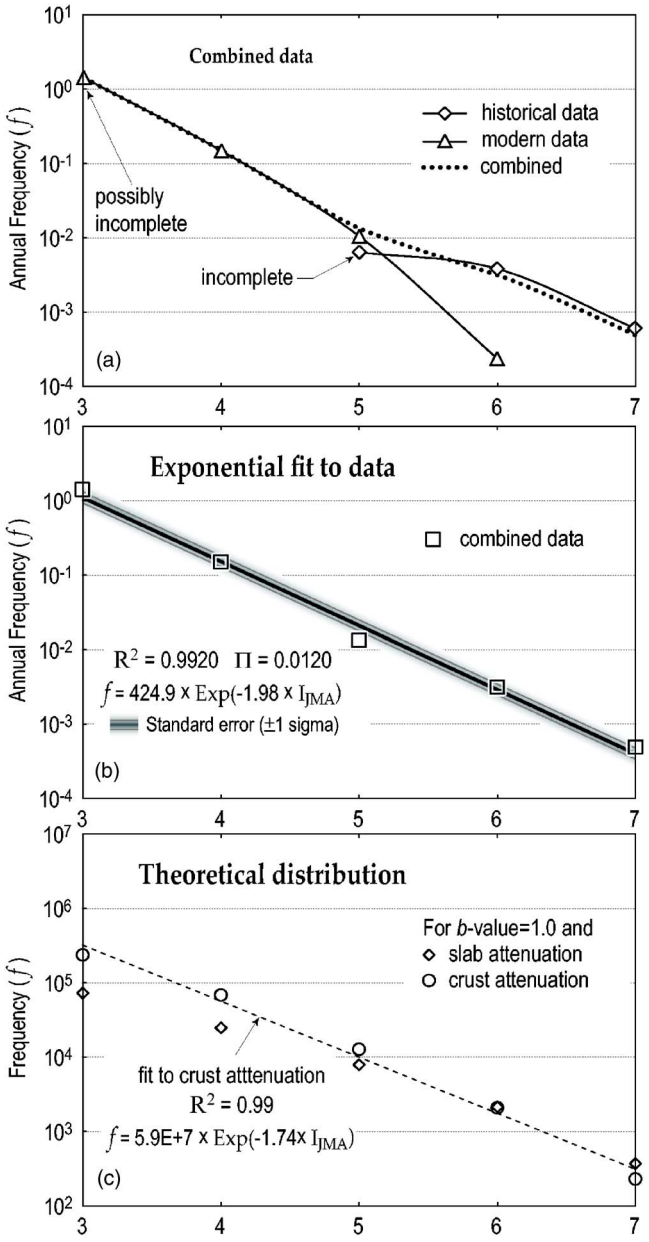

Figure 5. Frequency-intensity relation for the 10,416 combined observations, resembling the more familiar *b*-value (frequency-magnitude) relation. (a) Historical and modern data from Figure 2 are combined. (b) Fit of data to an exponential curve. (c) Theoretical distribution assuming a *b*-value of 1.0, a random distribution of $5 \geqslant M \geqslant 8$ earthquakes, and the Kanto regional attenuation relations for subduction slab and crustal earthquakes of Bakun (2005).

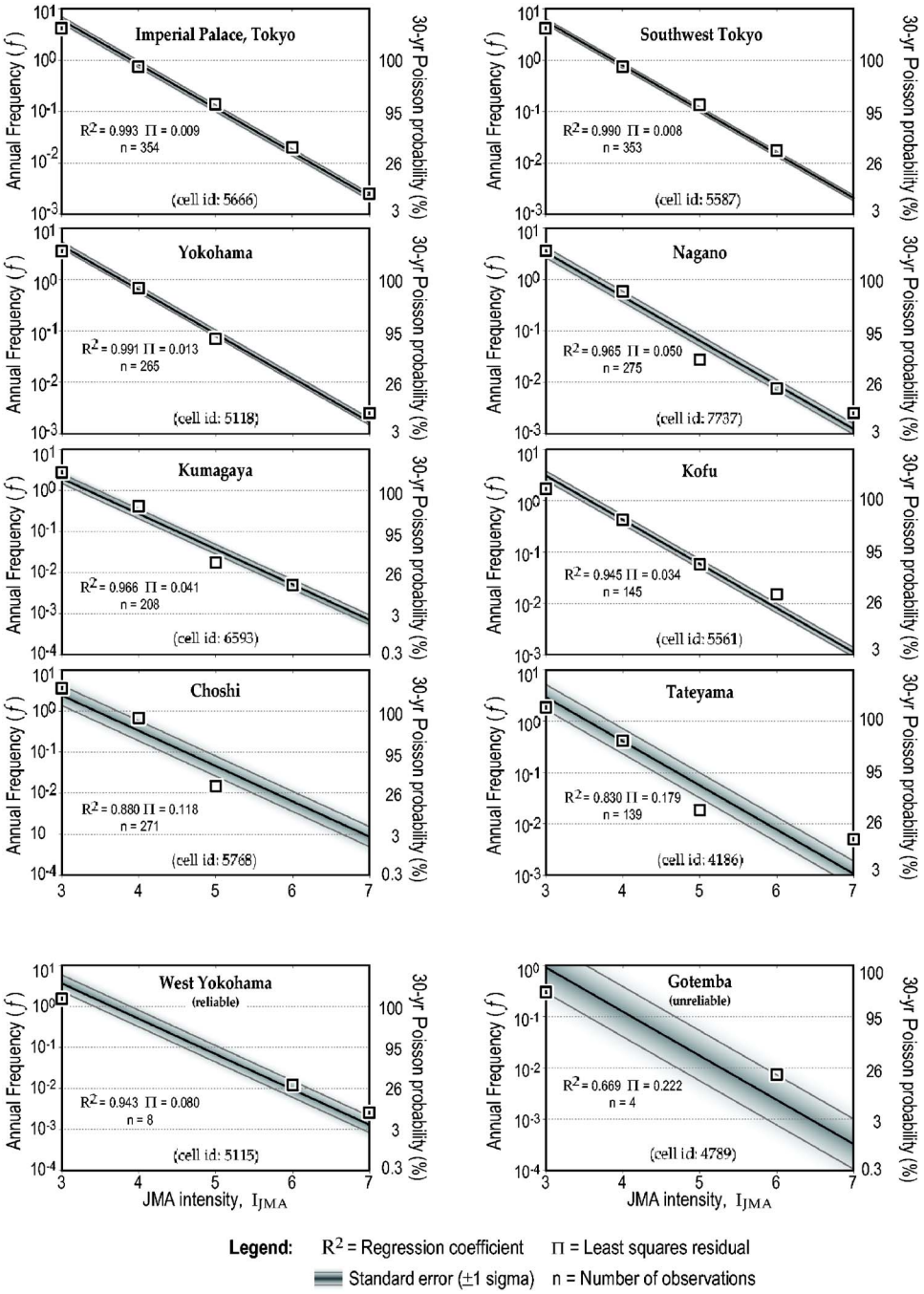

Figure 6. (a) Fit of the observations for eight cities to the regional slope, with only intercept determined locally; the regional slope found in Figure 5 is seen to fit the local data well. (b) West Yokohama and Gotemba are examples of cells with few observations; the former is deemed reliable and the latter unreliable.

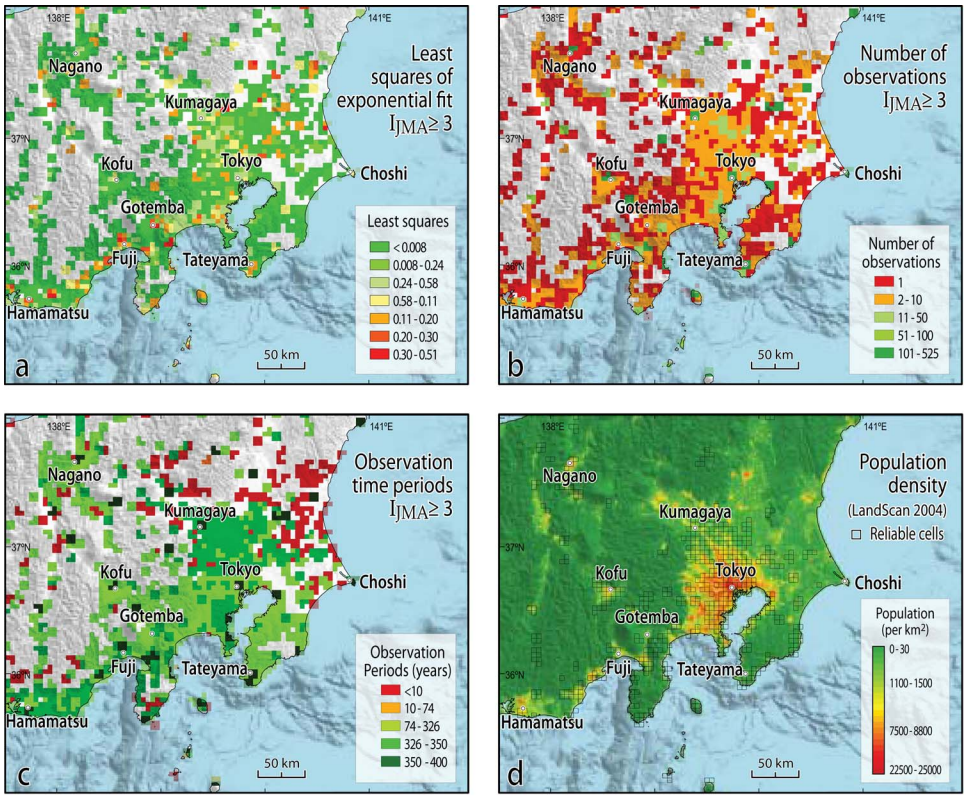

Figure 7. Three criteria used to evaluate cell reliability. (a) Least-squares residuals to the exponential fit. (b) The number of intensity observations. (c) The time period of the observations. (d) Cell coverage reflects the spatial distribution of population (Oak Ridge National Laboratory 2007). Although we lack uniform coverage, coverage is concentrated where people live.

CELL RELIABILITY

Significant portions of the Kanto area lack intensity observations. In addition, there are numerous cells with sparse data that do not fit the curves; an example, Gotemba, is shown in Figure 6b. We experimented with interpolation between reliable cells, but found that this tended to exaggerate areas of strong shaking. So we chose instead to omit cells without intensity observations, and to distinguish less reliable cells in the maps. Although this markedly reduces the area of coverage, we have observations wherever there is population (compare Figures 7b and 7d), and for the most part, this is where the earthquake hazard is most important.

Cell reliability is assessed by the goodness of fit to the model (Figure 7a), the number of observations (Figure 7b), and the time period covered (Figure 7c). This information is combined in the criteria to identify reliable cells: Data abundance criteria: ($[N_{\mathrm{IJMA}} \geqslant 50$ *or* $n_{\mathrm{IJMA}} \geqslant 3]$ and $[N_{\mathrm{IJMA}} = 5 \geqslant N_{\mathrm{IJMA}} \geqslant 6]$), or data consistency criteria:

([$\Pi < 0.1$ and $R^2 > 0.8$ and $N_{\mathrm{IJMA}} = 5 \geqslant N_{\mathrm{IJMA}} \geqslant 6$ and $N_{\mathrm{IJMA}} \geqslant 2$ and $t \geqslant 10$ yr])

$$R^2 = 1.0 - \left(\frac{\sum (\log(f_{observed}) - \log(f_{curvefit}))^2}{\sum (\log(f_{observed}) - \overline{(\log(f_{observed}))})^2} \right)$$

$$\Pi = \frac{\sum (\log(f_{observed}) - \log(f_{curvefit}))^2}{n_{IJMA}}$$

where N_{IJMA}=number of intensity observations, n_{IJMA}=number of intensity bins to run curve fit, R^2=regression coefficients, Π=least squares, t=observation time period, and f=annual frequency of the intensity level.

RESULTS

DISTRIBUTION OF SHAKING PROBABILITY

The frequency f of any JMA intensity can be transformed into a Poisson or time-averaged probability P for any time period t by $P = 1 - \exp(-ft)$. We use $\mathrm{I_{JMA}} = 6$ because it represents severe shaking and is well sampled by the data. The resulting 30-year probability of severe shaking is ~35% in the Tokyo-Kawasaki-Yokohama corridor, ~30% in Tateyama, ~15% in Choshi, and ~15% in Kumagaya (Figure 8a).

COMPARING OUR RESULTS TO GEOLOGY

Perhaps the strongest test of our results is whether the distribution of probability reflects the surficial geology and distribution of major faults (Figure 8c), since neither geology nor faults were imposed on the results or used in the calculations. In fact, we find a correlation between the probability and the presence or absence of stream deposits and bay mud, and between probability and proximity to the plate-boundary faults, which are the sources of the largest earthquakes (compare Figure 8a with 8b). To minimize sensitivity to outliers in the correlation, we consider all cells with probabilities ⩽45% and distances from the major faults ⩽150 km. A linear distance dependence accounting for 24% of the variance is found such that the probability at major faults is 16%, and 150 km away it is 6%. The mean shaking probability of cells in soft sediments is 19%, and for bedrock it is 14%.

TEST OF KEY ASSUMPTIONS

IS THE CATALOG TYPICAL OF LONG-TERM BEHAVIOR?

To use the observed record of shaking to estimate typical behavior, we must assess whether the 400-year period of intensity observations is sufficiently long. From the geodetically measured strain and vertical deformation during the past 15 years, Nishimura et al. (2007) inferred the seismic moment accumulation rate (the product of the cumulative fault slip rate, fault area, and crustal stiffness). Grunewald and Stein (2006) estimated the magnitude, location, and uncertainty of historical earthquakes since 1600, and performed a Monte Carlo simulation of the likely moment release rate associated with

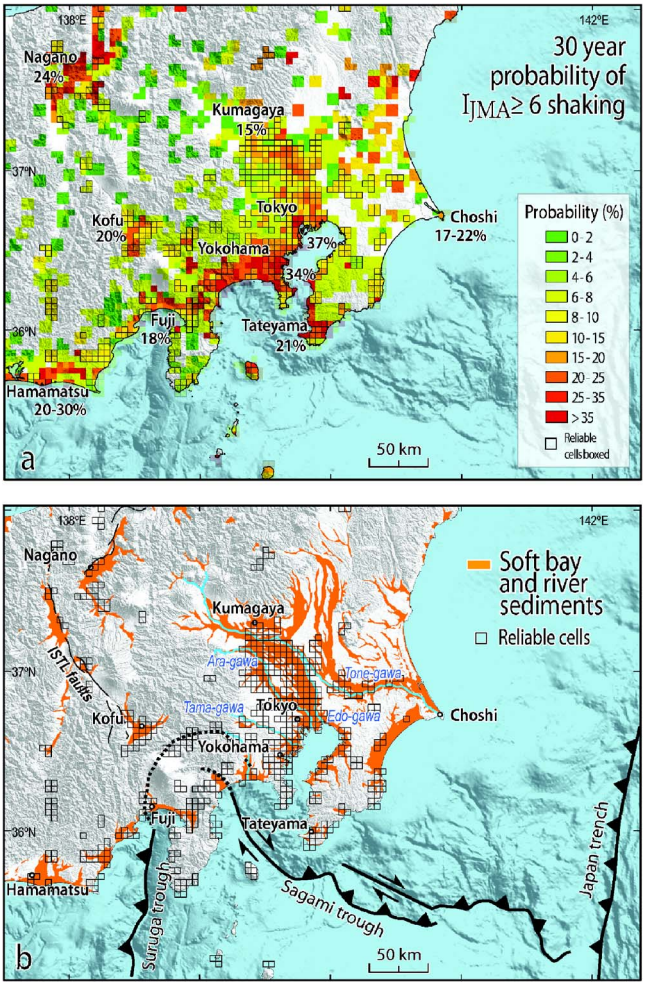

Figure 8. (a) The 30-year probability of JMA $I_{JMA} > 6$ shaking (equivalent to MMI > IX). Tokyo, Yokohama, and Nagano span multiple grid cells, and so percentages shown are average cells for those cities. (b) The shaking probability is higher in river sediments and bay mud; the probability increases with proximity to the major faults.

these earthquakes. Grunewald and Stein (2006) found the seismic release rate to be in close agreement with the moment accumulation rate. This means that the catalog is likely representative of the long-term process. Further, Shishikura (2003) and Shishikura et al. (in preparation) developed a record of 16 Sagami plate-boundary earthquakes during the past 7,200 years from uplifted marine terraces along the Boso peninsula, and Stein et al. (2006) used this record to infer a 403±66-year mean inter-event time for $M \geq 7.9$ events, about the time period of our intensity catalog. Thus, both analyses support our reliance on the 400-year catalog: the moment accumulation and release rates

are in balance, suggesting this period includes neither an earthquake deficit nor oversupply; and the catalog duration is roughly equal to the observed plate-boundary earthquake cycle, implying that the record likely encompasses the typical range of seismic behavior.

ARE THE INTENSITY DATA BIASED WITH TIME?

The second issue is whether there are systematic changes in the intensity standards because the observation density and spatial coverage increase with time, and because the building stock from which intensities are inferred changes with time. The best way to test this is to compare the intensities for two earthquakes of the same size and location that occurred centuries apart. Tsunami and marine terrace uplift data (Shishikura et al., in preparation) indicate that the 1923 Kanto and 1703 Genroku both slipped the two westernmost fault patches by the same amount; the difference between the events is that the 1703 shock slipped two additional patches to the east (compare Figure 1b with 1d). In Figures 9a and 9b we show the subset of cells with intensity observations for both events. Their resemblance is quite evident; the mean difference in intensity for these cells between 1703 and 1923 is only 0.26 intensity units. When comparing events with the same source, path, and site effects, attenuation Equation 8 of Bakun (2005) for the Kanto area subduction events reduces from

$$I_{PRED} = -8.33 + (2.19 \pm 0.32)M_{JMA} - 0.00550\Delta h - 1.14\, log\, \Delta h$$

to $d\mathrm{M_{JMA}} = d\mathrm{I_{JMA}}/(2.19 \pm 0.32)$, where $d\mathrm{M_{JMA}}$ is the difference between the two earthquake magnitudes, $d\mathrm{I_{JMA}}$ is the difference between the mean intensities, and Δh is in km. This results in an apparent JMA magnitude difference of 0.1 units for the 1703 versus 1923 earthquakes, in substantial agreement. Thus for the 200-year time span, intensities appear comparable, a testament to the work of Usami and Takemura.

We can also compare the 1855 M ~ 7.2 Ansei Edo earthquake intensities to that of the 23 July 2005 M = 6.0 Chiba shock that produced an intensity distribution similar to 1855 (Grunewald and Stein 2006), but with proportionally smaller values (Figure 9c and 9d). This similarity also argues that the past 150 years of intensities are comparable. The slope of the regression of all cells with both 1855 and 2005 observations is 0.7 (perfect agreement would yield 1.0), and the mean difference in intensities is 1.32 (in other words, a site with an intensity of 6 for 1855 corresponds to an intensity just below 5 in 2005). If we assume that the earthquakes share the same hypocenter, then using Equation 8 from Bakun (2005) for crustal earthquakes, $d\mathrm{M_{JMA}} = d\mathrm{I_{JMA}}/2.19$, and $d\mathrm{M_{JMA}} = 0.6 \pm 0.1$. So for 1855 Ansei-Edo, $\mathrm{M_{JMA}} = 6.6 \pm 0.1$. By comparison, Usami (2003) found M = 7.1, Bakun (2005) found M = 7.2, and Grunewald and Stein (2006) found M = 7.4.

ARE RESULTS TOO SENSITIVE TO KEY EARTHQUAKES?

The 1923 Kanto and 1855 Ansei-Edo earthquakes exert the largest influence on the probability maps. Stein et al. (2006) estimate an inter-event time of 403 ± 66 years for the Kanto earthquake and a more uncertain ~150 years for the Ansei-Edo earthquake, and so such events might be expected in a 400 year–long catalog drawn at random.

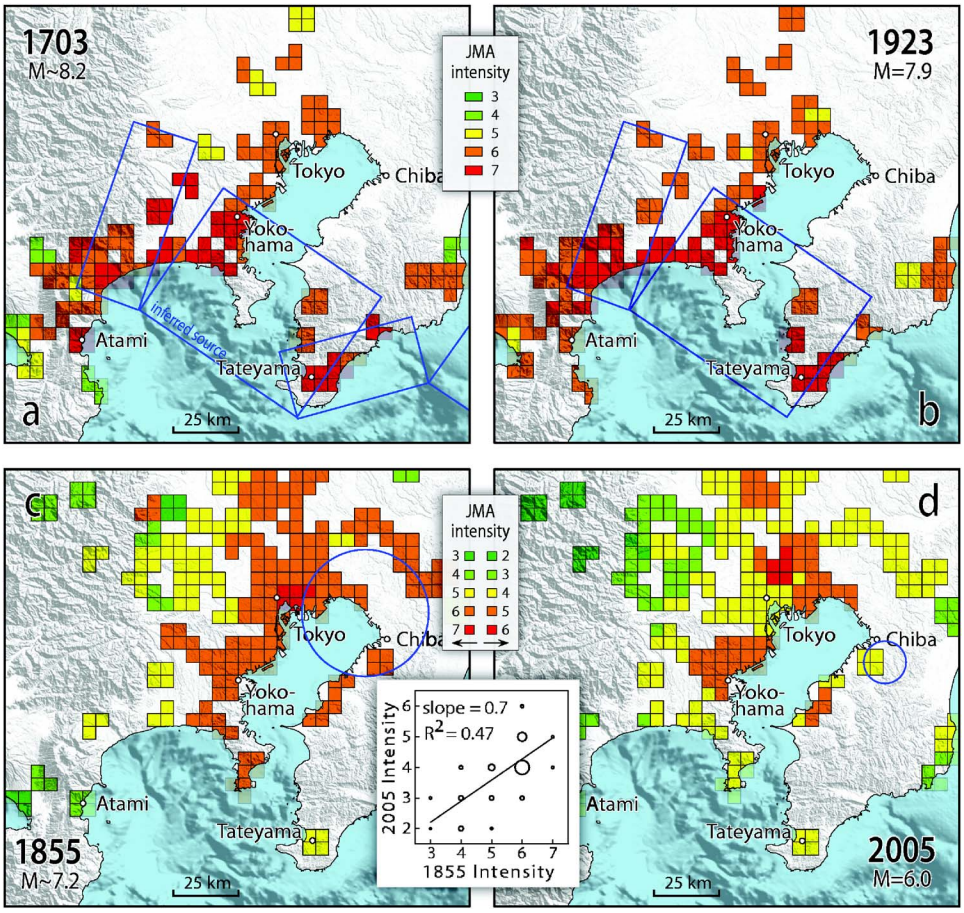

Figure 9. To assess systematic shifts in the intensity scale with time, we compare intensities for cells with observations from two earthquakes that struck 150–200 years apart. Intensities are plotted in the nearsource region that contains 70% of the common observations. (a) 1703 M ~8.2 Genroku earthquake intensities compared with (b) 1923 M=7.9 Kanto earthquake intensities. The mean difference in intensity is 0.26 intensity units, corresponding to 0.1 magnitude units. (c) 1855 Ansei-Edo earthquake intensities compared with (d) 2005 M=6.0 Chiba earthquake intensities. A regression on their intensities is inset (circle size is proportional to number of observations), with a slope close to 1.

The 1703 Genroku earthquake is more infrequent, with a ~2,200-year inter-event time (Shishikura 2003), but because of the paucity of 1703 intensity observations, it only modestly influences the probabilities. The Nagano region near the northwest corner of the map sustained the destructive 1847 Zenkoji M ~ 7.4 earthquake, which killed 8,000 people. An 1858 M ~ 7.0 earthquake also struck just outside of the western map border. Paleoseismic evidence suggests that the Nagano-Bonchi-Seien fault that ruptured in the 1847 earthquake has 800–2,500-year inter-event time (Earthquake Research Committee 2005), and so the 1847 event would not be typical of a 400-year catalog. We

Table 3. Probability of $I_{JMA} \leqslant 6$ shaking (PGA $\leqslant$ 0.4 g) in key cities

Site name	Cell ID	Longitude	Latitude	Number of observations	30-year Poisson probability (%)	
					Using all data	1703 & 1847 Eqs. removed
Tokyo	5666	139.76825	35.70035	354	38	35
SW Tokyo	5587	139.72333	35.66371	353	36	31
Yokohama	5118	139.67841	35.44348	265	30	14
Nagano	7737	138.19619	36.68335	275	23	16
Kumagaya	6593	139.36400	36.13878	208	14	13
Kofu	5561	138.55552	35.66371	145	22	18
Choshi	5768	140.84622	35.73698	271	17	14
Tateyama	4186	139.85808	35.00119	139	21	14
West Yokohama	5115	139.54367	35.44348	8	25	15
Gotemba	4789	138.91485	35.29632	4	7	5

thus repeated our analysis excluding intensity observations for the 1703 and 1847 earthquakes. When excluded, the $I_{JMA} \geqslant 6$ probability decreased 7% at Nagano, 6% at Yokohama, 4% at Kofu, 3% at Tokyo, and 1% at Kumagaya (Table 3). Thus our results are modestly sensitive to these two earthquakes.

DISCUSSION

COMPARISON TO OTHER STUDIES

Stein et al. (2006) analyzed the earthquake probability for Tokyo by relocating the historical earthquake catalog, associating earthquakes with faults, inferring the seismic slip rate of the fault sources, and estimating the inter-event time for the largest earthquakes. They found a 29% probability of earthquakes capable of producing $I_{JMA} \geqslant 6$ shaking in the Tokyo-Yokohama corridor, in good agreement with our findings here. The Japanese government issued a comprehensive study of the earthquake and shaking likelihood for all of Japan (Earthquake Research Committee 2005), publishing a map showing the time-dependent 30-year probability of $I_{JMA} \geqslant 6$ shaking for greater Tokyo (Figure 10). Because the digital files have not been published, we re-plotted the Tokyo portion of our map in the same probability color scale as that of the Earthquake Research Committee. Some 59% of the cells in both plots have the same probability level, and 98% are within one probability level. Thus, despite the large differences in approach, the probabilities are similar for Tokyo and its surrounding cities.

USE OF OUR RESULTS FOR BUILDING-CODE REGULATIONS

Regulators of building construction standards often base their codes on the level of shaking for which there is a 10% chance of exceedance in 50 years, roughly equivalent to the maximum shaking that might be observed in a 500-year period. We make such an

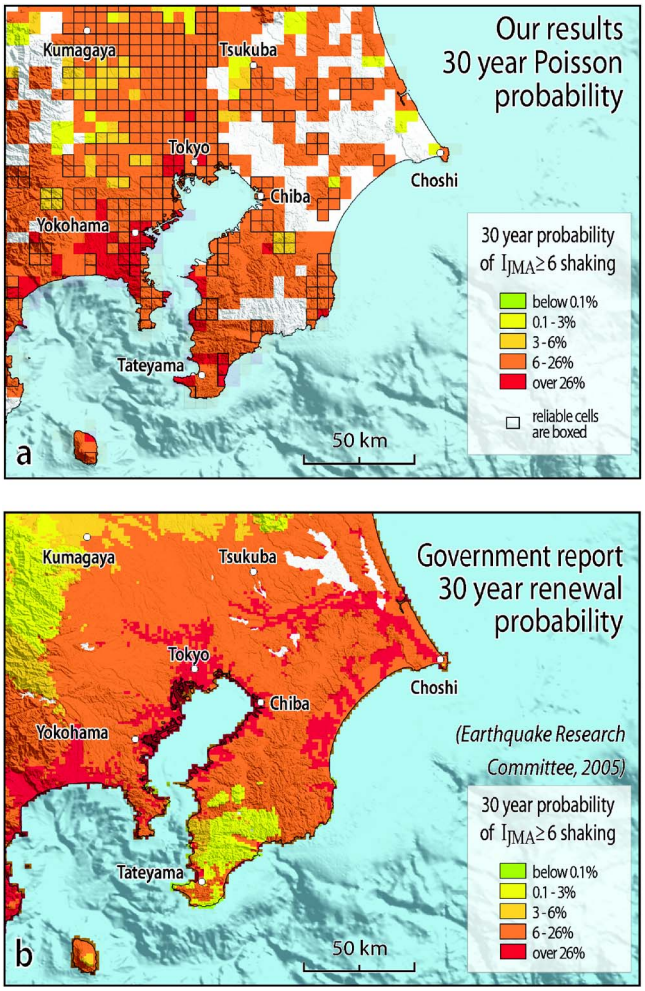

Figure 10. Using the probability scale adopted by the Earthquake Research Committee (2005), we re-plot our results for the immediate vicinity of Tokyo; results are similar for this region despite different approaches.

exceedance calculation in Figure 11a, based on the shaking frequency experienced in the past 400 years. This can be compared with the peak shaking observed during the past 400 years (Figure 1a). Not surprisingly, the two maps are similar. But there is more detail in the exceedance map because it is incremented in decimal JMA intensities, and because the exceedance map uses all observed intensities, whereas Figure 1a uses only the small subset of maximum observed intensities.

Our ability to transform the probability of a JMA intensity level into the probability of a peak ground acceleration (PGA) is dependent on large and damaging well-recorded calibration events with both instrumental and macroseismic intensities. The 23 October

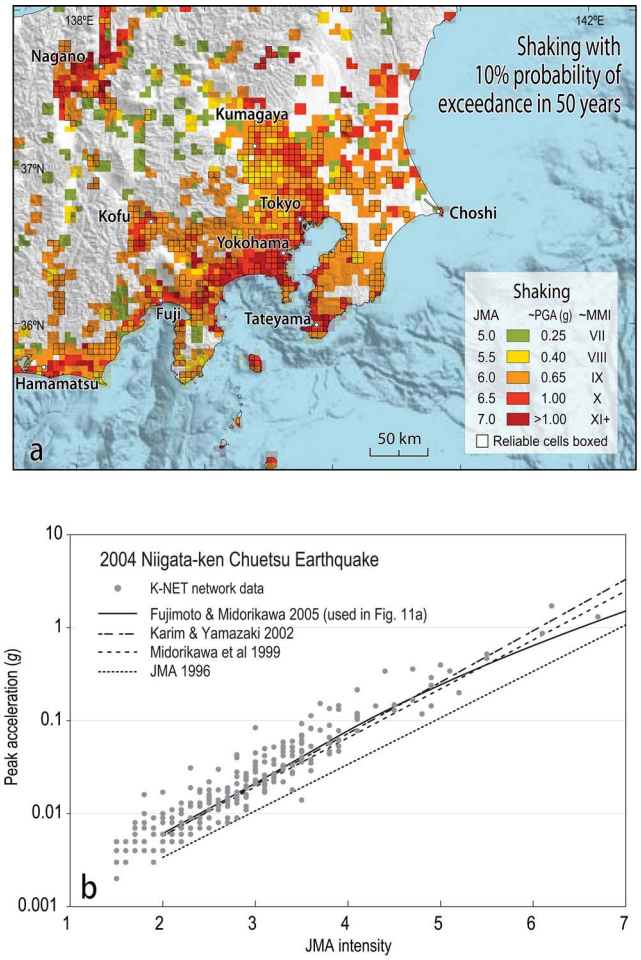

Figure 11. Map of the JMA intensity and PGA shaking (a) for which there is a 10% chance of exceedance in an average 50-year period, a criteria often used by building code regulators. Accelerations are most indicative of 6+2 Hz frequencies characteristic of one- to three-story buildings used to assess the intensities. In (b), 23 October 2004 Niigata-ken Chuetsu Earthquake strong motion, and intensity observations compared to the strong motion—intensity correlation models.

2004 Niigata-ken Chuetsu earthquake data (K-Net) provide such an essential calibration, because they sample JMA intensities from 1.5 to 6.5. In Figure 11b, intensity versus PGA correlation models by JMA (1996), Midorikawa et al. (1999), Karim and Yamazaki (2002), and Fujimoto and Midorikawa (2005) are compared with the Niigata-ken Chuetsu observations. We thus convert JMA intensities to ground accelerations using Fujimoto and Midorikawa (2005), which fits the full range of the data well, where:

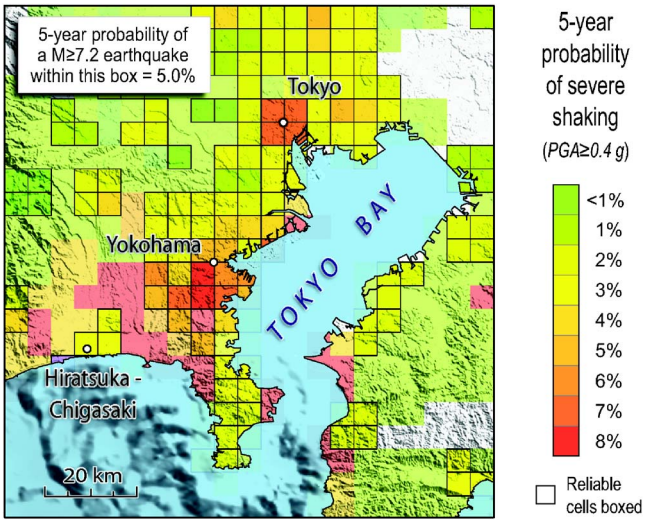

Figure 12. An illustration of a hypothetical catastrophe bond triggered by an earthquake of a given size and location (here, a $M \geq 7.2$ shock within the box), or by a specified level of observed shaking, equivalent to JMA intensity 6 and lower. The bond could be triggered by shaking in a restricted 5– × 5–km site, such as Tokyo Disneyland or the port of Yokohama, or it could be a regional average.

$$I_{\mathrm{JMA}} = 0.547 + 1.848 \log(\mathrm{PGA}) \pm 0.333 \text{ for } I_{\mathrm{JMA}} < 4 \text{ and}$$

$$I_{\mathrm{JMA}} = 1.905 + 0.381 \log(\mathrm{PGA}) + 0.384 \log(\mathrm{PGA})^2 \pm 0.379 \text{ for } I_{\mathrm{JMA}} \geq 4.$$

Given the nature of historical intensity observations on one- to three-story buildings, Figure 11a is most valid in the frequency range of 6±2 Hz (ICBO 1997).

USE OF OUR RESULTS FOR CATASTROPHE BONDS OR DERIVATIVES

Global reinsurance companies reduce their financial exposure by spreading risk among policies in many countries, and by transferring some risk to the much larger capital markets by issuing insurance-linked securities, known as catastrophe bonds. These bonds pay a high rate of quarterly interest unless the specified catastrophe occurs, in which case the investor could lose his or her principal. An earthquake catastrophe bond could be "triggered" by, among other things, an earthquake of a given magnitude falling into a specified location, or by shaking exceeding a specified threshold. Such bonds typically have maturities of less than a decade, and the investor must be able to assess the benefit of the high interest rate against the risk of losing the principal. Figure 12 shows a calculation for a hypothetical bond with a 5-year maturity. There is a 5% chance of a $M \geq 7.2$ shock striking somewhere within the box, a magnitude that Stein et al. (2006)

associate with $I_{JMA}=6$ (PGA $\sim$ 0.4 g) shaking. If the trigger were instead PGA $\geqslant$ 0.4 g shaking at a specific city, there is a 7% chance in central Tokyo, and an 8% chance in Yokohama.

APPLICATION OF THIS METHOD ELSEWHERE

At first glance, one might conclude that the intensity-based probability modeling we have presented is restricted to areas, such as Japan, that suffer frequent large earthquakes, but we suspect that this is not so. Instead, the sole requirements are a high spatial and temporal density of observations. In Italy, there are 35,000 observations recorded at 12,000 sites for 600 earthquakes for the period 461 BC through AD 1997 (Boschi et al. 2000). Equally important, there are 15 sites in Italy with more than 50 observations. So, despite a much lower rate of seismicity, Italy possesses three times Japan's number of observations. This is because in countries that rarely experience large earthquakes, people tend to report many more observations of small shocks. Because in our method the distribution of low intensities contributes to projection of the expected frequency of high intensities, a high rate of large earthquakes is not essential. Some other sites amenable to such an analysis include France (18,000 intensity observations of 33 earthquakes for the period 1866–2003 [Bakun and Scotti 2006]) and perhaps even California (52,000 MMI $\geqslant$3 observations of 7,900 earthquakes for the period 1769 to 1985 [NOAA/NGDC]).

CONCLUSIONS

Our argument is simply that the past frequency of shaking is very likely to be correlated with the future frequency of shaking, and so users can benefit from the opportunity to compare this approach with traditional probabilistic seismic analyses to make hazard judgments. The principal benefits of this approach are that it builds the fewest possible assumptions into a probabilistic seismic forecast, and that it includes site and source effects without imposing this behavior. The cost is that we must abandon any attempt to make a time-dependent forecast (describing the likelihood during the next 30 years, rather than during an average 30 years), which could be quite different. We believe the method is suitable to many applications of probabilistic seismic hazard analysis, and can be successfully applied to other countries and regions. At the very least, we view this data-rich method as an alternative that can be compared to assumption-rich approaches. In the Kanto region of Japan, the results are roughly equivalent to conventional seismic hazard analysis, and thus encouraging.

ACKNOWLEDGMENTS

We thank Emi Yarai for translation of Usami records and for laborious data conversion; Nobuo Hamada for the JMA intensity data set; Fred Pollitz, John Langbein, and Elliot Grunewald for advice; and William Bakun and John Boatwright for perceptive reviews. We gratefully acknowledge financial support from Swiss Re.

REFERENCES

Bakun, W. H., 2005. Magnitude and location of historical earthquakes in Japan and implications for the 1855 Ansei Edo earthquake, *J. Geophys. Res.* **110**, doi:10.1029/2004JB003329.

Bakun, W. H., and Scotti, O., 2006. Regional intensity attenuation models for France and the estimation of magnitude and location of historical earthquakes, *Geophys. J. Int.* **164**, 596–610.

Boschi, E., Guidoboni, E., Ferrari, G., Mariotti, D., Valensise, G., and Gasperini, P., 2000. Catalogue of strong Italian earthquakes from 461 B. C. to 1997, *Annali di Geofisica* 43, [CD-ROM].

Earthquake Research Committee, 2005. *Comprehensive Study of Probabilistic Seismic Hazard Map for Japan*, Headquarters for Earthquake Research Promotion, Tokyo.

Fujimoto, K., and Midorikawa, S., 2005. Empirical method for estimating J. M. A. instrumental seismic intensity from ground motion parameters using strong motion records during recent major earthquakes, *Regional Safe Academic Society Dissertation Collection* 7, [in Japanese].

Geological Survey of Japan, AIST, 2005. *Geologic Map of Japan, 1:1,000,000*, 3rd Edition, [CD-ROM version 2], Geological Survey of Japan, Ibaraki-ken.

Grunewald, E. D., and Stein, R. S., 2006. A new 1649–1884 catalog of destructive earthquakes near Tokyo and implications for the long-term seismic process, *J. Geophys. Res.* **111**, doi:10.1029/2005JB004059.

Hamada, N., Kazumitsu, Y., Nishwaki, M., and Abe, M., 2001. A comprehensive study of aftershocks of the 1923 Kanto earthquake, *Bull. Seismol. Soc. Jpn.* **54**, 251–265.

Headquarters for Earthquake Research Promotion, 2005. *Comprehensive Study of Probabilistic Seismic Hazard Map in Japan*, Headquarters for Earthquake Research Promotion Press, Japan. [available at: http://www.jishin.go.jp/main/chousa/05mar_yosokuchizu].

ICBO, 1997. *Uniform Building Code*, ISSN 0896-9655, International Conference of Building Officials, Chicago.

Japan Meteorological Agency, 1996. *Note on the JMA Seismic Intensity, Gyosei*, JMA Report 1996, Japan Meteorological Agency, Tokyo, [in Japanese].

——, 2004. *The Annual Seismological Bulletin 2002, 2004*, Japan Meteorological Agency, Tokyo, [CD-ROM].

Karim, K. R., and Yamazaki, F., 2002. Correlation of JMA instrumental seismic intensity with strong motion parameters, *Earthquake Eng. Struct. Dyn.* **31**, 1191–1212.

K-NET Kyoshin Network, NIED. *National Research Institute for Earth Science and Disaster Prevention*, Tennodai, Tsukuba-shi, Japan, [available at: www.k-net.bosai.go.jp].

Midorikawa, S., Fujimoto, K., and Muramatsu, I., 1999. Correlation of new J.M.A. instrumental seismic intensity with former J. M. A. seismic intensity and ground motion parameters, *J. Social Safety Sci.* **1**, 51–56, [in Japanese].

Miyazawa, M., and Mori, J., 2005. Recorded maximum seismic intensity maps in Japan from 1586 to 2004, *Seismol. Res. Lett.* **77**, 154–158.

Monachesi, G., Peruzza, L., Slejko, D., and Stucchi, M., 1994. Seismic hazard assessment using intensity point data, *Soil Dyn. Earthquake Eng.* **13**, 219–226.

National Geophysical Data Center (NGDC). *Online Earthquake Intensity Database*, National Oceanic and Atmospheric Administration, Washington, D.C., [available at: http://www.ngdc.noaa.gov/seg/hazard/int_srch.shtml].

Nishimura, T., Sagiya, T., and Stein, R. S., 2007. Crustal block kinematics and seismic potential of the northernmost Philippine Sea plate and Izu Microplate, central Japan, inferred from GPS and leveling data, *J. Geophys. Res.* **112**, doi:10.1029/2005JB004102.

Nyst, M., Nishimura, T., Pollitz, F. F., and Thatcher, W., 2006. The 1923 Kanto earthquake re-evaluated using a newly augmented geodetic data set, *J. Geophys. Res.* **111**, doi10.1029/2005JB003628.

Oak Ridge National Laboratory, 2004. *Landscan Global Population Database 2004*, University of Tennessee, Battelle, [available at: http://www.ornl.gov/gist/projects/LandScan/landscan_doc.htm].

Papoulia, J., and Slejko, D., 1997. Seismic hazard assessment in the Ionian islands based on observed macroseismic intensities, *Natural Hazards* **14**, 179–187.

Richter, C. F., 1958. *Elementary Seismology*, W. H. Freeman Company, San Francisco, pp. 135–149, 650–653.

Shabestaria, K. T., and Yamazaki, F., 2001. A proposal of instrumental seismic intensity scale compatible with MMI evaluated from three-component acceleration records, *Earthquake Spectra* **17**, 711–723.

Shishikura, M., 2003. Cycle of interplate earthquakes along the Sagami Trough deduced from tectonic geomorphology, *Bull. Earthquake Res. Inst., Univ. Tokyo* **78**, 245–254.

Shishikura, M., Toda, S., and Satake, K., 2007. Fault model of the 1703 Genoku Kanto earthquake (M 8.2) along the Sagami trough deduced from renewed coseismic crustal deformation, [in preparation].

Stein, R. S., Toda, S., Parsons, T., and Grunewald, E., 2006. A new probabilistic seismic hazard assessment for greater Tokyo, *Philo. Trans. R. Soc. A* **364**, 1965–1988.

Stirling, M., and Peterson, M., 2006. Comparison of the historical record of earthquake hazard with seismic-hazard models for New Zealand and the continental United States, *Bull. Seismol. Soc. Am.* **96**, 978–1994.

Takemura, M., and Moroi, T., 2001. Comprehensive list of the regional damage data sets for the 1923 Kanto earthquake, *J. Seismol. Soc. Jpn.* **53**, 285–302, [in Japanese].

Usami, T., 1994. *Seismic Intensity Maps and Isoseismal Maps of Historical Earthquakes of Japan*, Japan Electric Association, Tokyo.

——, 2003. *Materials Comprehensive List of Destructive Earthquakes in Japan, [416]—2001*, University of Tokyo Press, Japan.

Utsu, T., 1979. Seismicity of Japan from 1885 through 1925—a new catalog of earthquakes of $M \geqslant 6$ felt in Japan and smaller earthquakes which caused damage in Japan, *Bull. Earthquake Res. Inst., Univ. Tokyo* **54**, 253–308, [in Japanese].

——, 1982. Seismicity of Japan from 1885 through 1925, correction and supplement, *Bull. Earthquake Res. Inst., Univ. Tokyo* **57**, 111–117, [in Japanese].

——, 1988. A catalog of large earthquakes ($M \geqslant 6$) and damaging earthquakes in Japan for the years 1885–1925, in *Historical Seismograms and Earthquakes of the World*, edited by H. Meyers, K. Shimazaki, and B. Lee, Academic Press, San Diego, Calif., 150–161.

Wiemer, S., and Wyss, M., 1997. Mapping the frequency-magnitude distribution in asperities: an improved technique to calculate recurrence times?, *J. Geophys. Res.* **102**, 115–128.

(Received 26 July 2006; accepted 26 February 2007)